

Decays $Z \rightarrow e_a e_b$ in a 3-3-1 model with neutral leptons

T.T. Hong,^{1,2,*} L.T.T. Phuong,^{1,2,†} N.H.T. Nha,^{3,4,‡} and T. Phong Nguyen^{§5,¶}

¹*An Giang University, Long Xuyen City, Vietnam*

²*Vietnam National University, Ho Chi Minh City, Vietnam*

³*Subatomic Physics Research Group,*

Science and Technology Advanced Institute,

Van Lang University, Ho Chi Minh City, Vietnam

⁴*Faculty of Applied Technology, School of Technology,*

Van Lang University, Ho Chi Minh City, Vietnam

⁵*Department of Physics, Can Tho University, 3/2 Street, Can Tho, Vietnam*

Abstract

We investigate the 3-3-1 model with neutral leptons (called the 331NL for short) and by that, we will point out that this model can simultaneously explain the lepton flavor violating (LFV) decays of the Z boson $Z \rightarrow e_a e_b$, Standard model-like Higgs boson decay $h \rightarrow e_b e_a$, and the charged leptons $e_b \rightarrow e_a \gamma$ consistent with the recent experimental data. In addition, the numerical results show strict relations among these decay rates of Z and h which are predicted by this model. As a result, the decay channels can be determined theoretically if one of them is detected by experiments.

PACS numbers:

§ Corresponding author

*Electronic address: tthong@agu.edu.vn

†Electronic address: lttphuong@agu.edu.vn

‡Electronic address: nguyenhuathanhnha@vlu.edu.vn

¶Electronic address: thanhphong@ctu.edu.vn

I. INTRODUCTION

We will use results of the general one-loop contributions to the LFV decay amplitudes of the Z boson (LFVZ) [1] to study a particular case of the $331NL$. The $331NL$ with inverse seesaw (ISS) neutrino can explain successfully all of the neutrino oscillation data, the data of LFV of the charged leptons (cLFV) decay $e_b \rightarrow e_a \gamma$, and SM-like Higgs boson (LFVh) decay $h \rightarrow \tau e, \tau \mu$, which can reach values of $\mathcal{O}(10^{-4})$ [2]. However, the LFVZ decay channel has not yet been implemented in the $331NL$ model. We hope that there are possibilities for signals of LFVZ decay in the allowed regions accommodating the other LFV data in $331NL$ models with ISS neutrinos. It was shown previously that if all heavy ISS neutrino have the same masses, the strict relations between three cLFV decay rates $\text{Br}(e_b \rightarrow e_a \gamma)$ will predict invisible signals of the two decays $\tau \rightarrow e \gamma, \mu \gamma$ in the near future [3]. In this work, we consider the more general situation of different masses for ISS neutrinos, so that all cLFV decay rates will reach the recent and future experimental sensitivities. Two other processes, LFVZ and LFVh decays will be discussed simultaneously to guarantee whether their decay rates are excluded, invisible, or still promising for the searching from the incoming experiments.

LFVZ decay have been investigated in many Beyond the Standard Models (BSM) which produced large LFVZ but small LFVh decay rates [4]. Similarly, the 2HDM (Two-Higgs Doublet Model) with ISS neutrinos predicts the $\text{Br}(Z \rightarrow \mu^\pm \tau^\mp) \sim \mathcal{O}(10^{-8})$ are large value but restrained value of $\text{Br}(h \rightarrow \mu^\pm e^\mp) < 10^{-8}$ [5]. However, the predictions from another 2HDM, as discussed in Ref. [6], present a contrasting viewpoint, which predicts larger values of LFVh and smaller values of LFVZ decay rates. Studies of the LFVZ decay channels can contribute to find new signals of physics. Our results are expected to be consistent with the latest experimental value's bounds for the LFVZ decays and satisfy the constraint condition for the other decay channels such as cLFV, LFVh, ... based on recent researchs on the LFVZ decay channel, named the 2HDM, 3-3-1 model [1, 5–7]. We will show that the $331NL$ can explain LFVZ, and satisfy the constraint of cLFV and LFVh decay.

The LFVZ decays have been recently paid attention both sides of lepton flavor violating (LFV) [8–10]. The LFVZ decay rates are constrained by recent experimental as $\text{Br}(Z \rightarrow \tau^\pm e^\mp) < 5.0 \times 10^{-6}$ [11], $\text{Br}(Z \rightarrow \tau^\pm \mu^\mp) < 6.5 \times 10^{-6}$ [11], and $\text{Br}(Z \rightarrow \mu^\pm e^\mp) < 2.62 \times 10^{-7}$ [12]. Additionally, the projected sensitivities for future experiments are as follows: at HL-LHC [13] with 10^{-6} , 10^{-6} , and 7×10^{-8} ; and at FCC-ee [13, 14] with 10^{-9} , 10^{-9} , and

10^{-10} , respectively.

The structure of this work is organized as follows. In section II, we will review the necessary components of the $331NL$ for study $Z \rightarrow e_a e_b$ decay and how the ISS framework can produce the active neutrino masses and mixing coherent with the experimental data. We will also discuss on the one-loop contributions to the decay amplitudes $Z \rightarrow e_b e_a$. The couplings and analytic formulas related to LFVZ decay will be determined in section III. In next section (section IV), we will examine the decay $Z \rightarrow e_b e_a$, concentrating on the areas of the parameter region content in the 1σ range of the LFV experimental data. In section V, the crucial results are summarized and presented in our conclusions. Finally, Appendix A shows the master functions of the one-loop contribution to LFVZ decay amplitudes in the unitary gauge.

II. THE 3-3-1 MODEL WITH NEUTRAL LEPTON

A. Particle content and neutrino masses from the ISS mechanism

We only focus on particle spectrum of the $331NL$ model which is necessary to this work. The detail discussions can be find in the previous papers [3, 15, 17] which is irrelevant with our study so we will ignore here. $Q = T_3 - \frac{T_8}{\sqrt{3}} + X$ is the electric charge operator which is identified by the gauge group $SU(3)_L \times U(1)_X$, in which $T_{3,8}$ are diagonal $SU(3)_L$ generators. Each lepton generation contains a $SU(3)_L$ triplet $L_{aL} = (\nu_a, e_a, N_a)_L^T \sim (3, -\frac{1}{3})$, $e_{aR} \sim (1, -1)$ which is a RH (right-handed) charged lepton, and a new neutral lepton $X_{aR} \sim (1, 0)$ with $a = 1, 2, 3$. The three Higgs triplets of the model are $\rho = (\rho_1^+, \rho^0, \rho_2^+)^T \sim (3, \frac{2}{3})$, $\eta = (\eta_1^0, \eta^-, \eta_2^0)^T \sim (3, -\frac{1}{3})$, and $\chi = (\chi_1^0, \chi^-, \chi_2^0)^T \sim (3, -\frac{1}{3})$. All quark and lepton masses at tree-level are generated by the vacuum expectation values (vev) are $\langle \rho \rangle = (0, \frac{v_1}{\sqrt{2}}, 0)^T$, $\langle \eta \rangle = (\frac{v_2}{\sqrt{2}}, 0, 0)^T$ and $\langle \chi \rangle = (0, 0, \frac{w}{\sqrt{2}})^T$. Two neutral Higgs components have zero vevs due to they have non-zero lepton numbers [17], when the model respects an $U(1)_\mathcal{L}$ defined as the generalized lepton number [18].

The covariant kinetic Lagrangian of the Higgs boson triplets generates mass for nine gauge bosons $\mathcal{L}^\phi = \sum_{\phi=\chi, \eta, \rho} (D_\mu \phi)^\dagger (D^\mu \phi)$, where $D_\mu = \partial_\mu - igW_\mu^a T^a - ig_X T^9 X X_\mu$, $a = 1, 2, \dots, 8$, and $T^9 \equiv \frac{I_3}{\sqrt{6}}$ and $\frac{1}{\sqrt{6}}$ corresponding to (anti)triplets and singlets [22]. The matrix $W^a T^a$

can be presented as

$$W_\mu^a T^a = \frac{1}{2} \begin{pmatrix} W_\mu^3 + \frac{1}{\sqrt{3}} W_\mu^8 & \sqrt{2} W_\mu^+ & 0 \\ \sqrt{2} W_\mu^- & -W_\mu^3 + \frac{1}{\sqrt{3}} W_\mu^8 & \sqrt{2} Y_\mu^+ \\ 0 & \sqrt{2} Y_\mu^- & -\frac{2}{\sqrt{3}} W_\mu^8 \end{pmatrix}, \quad (1)$$

where $T^a = \lambda_a/2$ respective to a triplet representation. The model consists of W^\pm and Y^\pm which are two pairs of singly charged gauge bosons as follows

$$W_\mu^\pm = \frac{1}{\sqrt{2}}(W_\mu^1 \mp iW_\mu^2), \quad Y_\mu^\pm = \frac{1}{\sqrt{2}}(W_\mu^6 \pm iW_\mu^7), \quad (2)$$

with the respective masses $m_W^2 = \frac{g^2}{4}(v_1^2 + v_2^2)$ and $m_Y^2 = \frac{g^2}{4}(w^2 + v_1^2)$. The model will be broken step by step as $SU(3)_L \times U(1)_X \rightarrow SU(2)_L \times U(1)_Y \rightarrow U(1)_Q$, leading to identify W^\pm as the SM ones, therefore the following relations are obtained

$$v_1^2 + v_2^2 \equiv v^2 = (246\text{GeV})^2, \quad \frac{g_X}{g} = \frac{3\sqrt{2}s_W}{\sqrt{3-4s_W^2}}, \quad g = e/s_W, \quad (3)$$

where e and s_W are the electric charge and sine of the Weinberg angle $s_W^2 \simeq 0.231$, respectively. Similarly to the 2HDM, the following parameters will be used

$$t_\beta \equiv \tan \beta = \frac{v_2}{v_1}, \quad v_1 = c_\beta \times v, \quad v_2 = s_\beta \times v. \quad (4)$$

The lepton masses generated from the Yukawa Lagrangian are below

$$\mathcal{L}_l^Y = -h_{ab}^e \bar{L}_a \rho e_{bR} + h_{ab}^\nu \epsilon^{ijk} \overline{(L_a)_i} (L_b)_j^c \rho_k^* - y_{ba}^X \overline{X_{bR}} \chi^\dagger L_a - \frac{1}{2} (\mu_X)_{ab} \overline{X_{aR}} (X_{bR})^c + \text{h.c.}, \quad (5)$$

where $a, b = 1, 2, 3$. The charged lepton masses generated from the first term of Eq. (5) as $m_{e_a} \equiv \frac{h_{ab}^e v_1}{\sqrt{2}} \delta_{ab}$, which we presume the flavor states are physical.

In the basis $n'_L = (\nu_L, N_L, (X_R)^c)^T$, the Lagrangian (5) gives a neutrino mass term with the total 9×9 mass matrix written in terms of the following block form of 3×3 sub-matrices [15]

$$-\mathcal{L}_{\text{mass}}^\nu = \frac{1}{2} \overline{(n'_L)^c} \mathcal{M}^\nu n'_L + \text{h.c.}, \quad \text{where} \quad \mathcal{M}^\nu = \begin{pmatrix} \mathcal{O}_3 & m_D^T & \mathcal{O}_3 \\ m_D & \mathcal{O}_3 & M_R^T \\ \mathcal{O}_3 & M_R & \mu_X \end{pmatrix}, \quad (6)$$

where $(n'_L)^c = ((\nu_L)^c, (N_L)^c, X_R)^T$, $(M_R)_{ab} \equiv y_{ab}^X \frac{w}{\sqrt{2}}$, and $(m_D^T)_{ab} = -(m_D)_{ab} \equiv \sqrt{2} h_{ab}^\nu v_1$ with $a, b = 1, 2, 3$. The matrix μ_X in Eq. (5) is symmetric, then we consider this matrix as diagonal, which simplifies the calculations without loss of generality.

By using the 9×9 unitary matrix U^ν that can diagonalize mass matrix \mathcal{M}^ν as follow

$$U^{\nu T} \mathcal{M}^\nu U^\nu = \hat{M}^\nu = \text{diag}(m_{n_1}, m_{n_2}, \dots, m_{n_9}) = \text{diag}(\hat{m}_\nu, \hat{M}_N), \quad (7)$$

where the physical states n_{iL} have masses corresponding to m_{n_i} ($i = 1, 2, \dots, 9$). The two mass matrices $\hat{m}_\nu = \text{diag}(m_{n_1}, m_{n_2}, m_{n_3})$ and $\hat{M}_N = \text{diag}(m_{n_4}, m_{n_5}, \dots, m_{n_9})$ corresponding to the active extra neutrinos n_{aL} ($a = 1, 2, 3$) and n_{IL} ($I = 1, 2, \dots, 6$), respectively. The following approximate solution for the neutrino mixing matrix U^ν is reasonable for any particular seesaw mechanisms,

$$U^\nu = \Omega \begin{pmatrix} U_{\text{PMNS}} & \mathcal{O}_{3 \times 6} \\ \mathcal{O}_{6 \times 3} & V \end{pmatrix}, \quad \Omega \simeq \begin{pmatrix} I_3 - \frac{1}{2} R R^\dagger & R \\ -R^\dagger & I_6 - \frac{1}{2} R^\dagger R \end{pmatrix}, \quad (8)$$

where R, V are $3 \times 6, 3 \times 6$ matrices, respectively. To derive the ISS relations perturbatively, it is assumed that all entries of the matrix R satisfy $|R_{aI}| \ll 1$.

The flavor and mass eigenstates are shown through the relations below

$$n'_L = U^\nu n_L, \quad \text{and } (n'_L)^c = U^{\nu*} (n_L)^c \equiv U^{\nu*} n_R, \quad (9)$$

where $n_L \equiv (n_{1L}, n_{2L}, \dots, n_{9L})^T$, and n_i represents the Majorana states with components $(n_{iL}, n_{iR})^T$.

We summarize here the ISS expressions:

$$R_2^* = m_D^T M_R^{-1}, \quad R_1^* = -R_2^* \mu_X (M_R^T)^{-1} \simeq \mathcal{O}_3, \quad (10)$$

$$m_\nu = R_2^* \mu_X R_2^\dagger = U_{\text{PMNS}}^* \hat{m}_\nu U_{\text{PMNS}}^\dagger = m_D^T M_R^{-1} \mu_X (M_R^{-1})^T m_D, \quad (11)$$

$$V^* \hat{M}_N V^\dagger = M_N + \frac{1}{2} M_N R^\dagger R + \frac{1}{2} R^T R^* M_N. \quad (12)$$

All independent parameters $x_{12,13}$ and three entries of $M^{-1} \equiv M_R^{-1} \mu_X (M_R^{-1})^T$ can be determined from experimental data of m_ν [3, 15], particular the Dirac mass matrix exhibits an antisymmetric structure as follows

$$m_D = z e^{i\alpha_{23}} \times \tilde{m}_D, \quad \text{where } \tilde{m}_D = \begin{pmatrix} 0 & x_{12} & x_{13} \\ -x_{12} & 0 & 1 \\ -x_{13} & -1 & 0 \end{pmatrix}, \quad (13)$$

where $\alpha_{23} \equiv \arg[h_{32}^\nu]$ and

$$z = \sqrt{2} |h_{32}^\nu| v_1 = \sqrt{2} |h_{23}^\nu| v_1 \equiv c_\beta z_0 \quad (14)$$

is a real and positive parameter. The Eq. (11) gives $(m_\nu)_{ij} = [m_D^T M^{-1} m_D]_{ij}$ for all $i, j = 1, 2, 3$, cause to six independent functions. Inserting $(m_\nu)_{ij}$ into the three remaining relations with $i = j$, we obtain

$$x_{12} = \frac{(m_\nu)_{12} (m_\nu)_{13} - (m_\nu)_{11} (m_\nu)_{23}}{(m_\nu)_{13} (m_\nu)_{23} - (m_\nu)_{12} (m_\nu)_{33}}, \quad x_{13} = \frac{(m_\nu)_{13}^2 - (m_\nu)_{11} (m_\nu)_{33}}{(m_\nu)_{13} (m_\nu)_{23} - (m_\nu)_{12} (m_\nu)_{33}}, \quad (15)$$

and $\text{Det}[m_\nu] = 0$. We express all parameter of the matrix μ_X as certain but lengthy functions of $(ze^{i\alpha_{32}})$, all entries of M_R and m_ν by using $M^{-1} = M_R^{-1} \mu_X (M_R^{-1})^T$. While experiment data help to determine m_ν , others are free parameters. We choose $\alpha_{32} = 0$, because it is absorbed into the μ_X .

We consider in the limit that $|R_2| \ll 1$, based on Eq. (12), we can determine approximately the heavy neutrino masses, namely

$$V^* \hat{M}_N V^\dagger \simeq M_N. \quad (16)$$

For convenience, we identify the reduced matrix:

$$M_R \equiv ze^{i\alpha_{23}} \tilde{M}_R, \quad (\tilde{M}_R)_{ij} \equiv k_{ij}, \quad (17)$$

so that $R_2^* = -\tilde{m}_D / \tilde{M}_R$. Since the matrix M_R is always diagonalized by two unitary transformations V_L and V_R [16],

$$V_L^T M_R V_R = z \times \hat{k} = z \times \text{diag}(\hat{k}_1, \hat{k}_2, \hat{k}_3), \quad (18)$$

where all $\hat{k}_{1,2,3}$ are always positive, $\hat{k}_a \gg 1$ so that all ISS relations are valid. Therefore, M_R is determined in terms of free parameters included in \hat{k} , $V_{L,R}$. Based on Eq. (12), we can prove that the matrix V can be determined approximately as follows

$$V = \frac{1}{\sqrt{2}} \begin{pmatrix} V_R & iV_R \\ V_L & -iV_L \end{pmatrix} \rightarrow V^T M_N V = z \times \begin{pmatrix} \hat{k} & \mathcal{O}_{3 \times 3} \\ \mathcal{O}_{3 \times 3} & \hat{k} \end{pmatrix}. \quad (19)$$

Consequently, for any qualitative estimations, by using the crude approximations that heavy neutrinos masses are $m_{n_{a+3}} = m_{n_{a+6}} \simeq z \hat{k}_a$ with $a=1,2,3$; $R_1 \simeq \mathcal{O}_3$; and

$$U^\nu \simeq \begin{pmatrix} \left(I_3 - \frac{1}{2} R_2 R_2^\dagger \right) U_{\text{PMNS}} & \frac{1}{\sqrt{2}} R_2 V_L & \frac{-i}{\sqrt{2}} R_2 V_L \\ \mathcal{O}_3 & \frac{V_R}{\sqrt{2}} & \frac{iV_R}{\sqrt{2}} \\ -R_2^\dagger U_{\text{PMNS}} & \left(I_3 - \frac{R_2^\dagger R_2}{2} \right) \frac{V_R}{\sqrt{2}} & \left(I_3 - \frac{R_2^\dagger R_2}{2} \right) \frac{-iV_R}{\sqrt{2}} \end{pmatrix}. \quad (20)$$

We have verified that the approximations mentioned give numerical results appropriate to the numerical calculations discussed in Ref. [17]. Therefore, in this work, we employ approximate formulas. The input value for the neutrino mass m_ν is chosen based on the 3σ neutrino oscillation data to determine \tilde{m}_D . We investigate the parameter space by scanning the free parameters z_0 and $\hat{k}_{1,2,3}$, V_R within reasonable ranges. Using these values, we construct the total neutrino mixing matrix U^ν , as defined in Eq. (20). Because V_L satisfies that

$$R_2 V_L = \tilde{m}_D^\dagger V_R^* \hat{k}^{-1}, \quad R_2 R_2^\dagger = \tilde{m}_D^\dagger V_R \hat{k}^{-2} \tilde{m}_D, \quad (21)$$

which is independent explicitly on V_L . Hence all processes we discuss here are weakly affected by V_L . We then will be fixed at $V_L = I_3$ from here to the end of this study.

According from Ref. [18], lagrangian for quark masses were presented. In this work, it is important to emphasize that the perturbative limit $h_{33}^u < \sqrt{4\pi}$ is required for the Yukawa couplings of the top quark must satisfy, which imposes a lower bound on v_2 : $v_2 > \frac{\sqrt{2}m_t}{\sqrt{4\pi}}$. By combine with the relationship in Eqs. (3) and (4), as results that $t_\beta \geq 0.3$. From the tau mass, $m_\tau = h_{33}^3 \times v c_\beta \sqrt{2} \rightarrow h_{33}^3 = m_\tau \sqrt{2} / (v c_\beta) < \sqrt{4\pi}$ can derived the upper bound of t_β , resulting in a rather weak upper bound $t_\beta = \sqrt{1/c_\beta^2 - 1} \leq 346$.

B. Higgs bosons

In this work, the Higgs potential respects the new lepton number identified in Ref. [18], namely

$$V_{higgs} = \sum_{\phi} \left[\mu_\phi^2 \phi^\dagger \phi + \lambda_\phi (\phi^\dagger \phi)^2 \right] + \lambda_{12} (\eta^\dagger \eta) (\rho^\dagger \rho) + \lambda_{13} (\eta^\dagger \eta) (\chi^\dagger \chi) + \lambda_{23} (\rho^\dagger \rho) (\chi^\dagger \chi) \\ + \tilde{\lambda}_{12} (\eta^\dagger \rho) (\rho^\dagger \eta) + \tilde{\lambda}_{13} (\eta^\dagger \chi) (\chi^\dagger \eta) + \tilde{\lambda}_{23} (\rho^\dagger \chi) (\chi^\dagger \rho) + \sqrt{2} \omega f (\epsilon_{ijk} \eta^i \rho^j \chi^k + \text{h.c.}), \quad (22)$$

where f is a dimensionless term, $\phi = \eta, \rho, \chi$. The general lepton number \mathcal{L} is broken softly by these three trilinear couplings. In previous research, the minimum conditions of the Higgs potential and the identification of the SM-like Higgs boson were thoroughly examined, as seen in references such as [19, 20]. Here, we summarize the essential results: The 331NL model includes two pairs of singly charged Higgs boson, denoted as h_1^\pm, h_2^\pm , along with two Goldstone bosons $G_{W,Y}^\pm$ of the singly charged gauge bosons W^\pm , and Y^\pm , respectively. $m_{h_1^\pm}^2 = \left(\frac{\tilde{\lambda}_{12} v^2}{2} + \frac{f w^2}{s_\beta c_\beta} \right)$, $m_{h_2^\pm}^2 = (v^2 c_\beta^2 + w^2) \left(\frac{\tilde{\lambda}_{23}}{2} + f t_\beta \right)$, and $m_{G_W}^2 = m_{G_Y}^2 = 0$. The original

and mass eigenstates of the charged Higgs bosons are described in Ref.[19] as

$$\begin{pmatrix} \eta^\pm \\ \rho_1^\pm \end{pmatrix} = \begin{pmatrix} -s_\beta & c_\beta \\ c_\beta & s_\beta \end{pmatrix} \begin{pmatrix} G_W^\pm \\ h_1^\pm \end{pmatrix}, \quad \begin{pmatrix} \rho_2^\pm \\ \chi^\pm \end{pmatrix} = \begin{pmatrix} -s_{13} & c_{13} \\ c_{13} & s_{13} \end{pmatrix} \begin{pmatrix} G_Y^\pm \\ h_2^\pm \end{pmatrix}, \quad (23)$$

where $t_{13} = v_1/w$, and

$$f = \frac{c_\beta s_\beta (2m_{h_1^\pm}^2 - \tilde{\lambda}_{12}v^2)}{2\omega^2}. \quad (24)$$

Three neutral gauge bosons are predicted by this model, where there is one zero eigenvalue corresponding to the massless photon. Defining [22]

$$s_{331} \equiv \sin \theta_{331} = \sqrt{1 - \frac{t_W^2}{3}}, \quad c_{331} \equiv \cos \theta_{331} = -\frac{t_W}{\sqrt{3}}, \quad (25)$$

The original and physical basis of the neutral gauge bosons are presented below

$$\begin{pmatrix} X_\mu \\ W_\mu^3 \\ W_\mu^8 \end{pmatrix} = \begin{pmatrix} s_{331} & 0 & c_{331} \\ 0 & 1 & 0 \\ c_{331} & 0 & -s_{331} \end{pmatrix} \begin{pmatrix} c_W & -s_W & 0 \\ s_W & c_W & 0 \\ 0 & 0 & 1 \end{pmatrix} \begin{pmatrix} 1 & 0 & 0 \\ 0 & c_\theta & -s_\theta \\ 0 & s_\theta & c_\theta \end{pmatrix} \begin{pmatrix} A_\mu \\ Z_{1\mu} \\ Z_{2\mu} \end{pmatrix} = C \begin{pmatrix} A_\mu \\ Z_{1\mu} \\ Z_{2\mu} \end{pmatrix}, \quad (26)$$

$$C = \begin{pmatrix} s_{331}c_W & (-s_{331}s_Wc_\theta + c_{331}s_\theta) & (s_{331}s_Ws_\theta + c_{331}c_\theta) \\ s_W & c_Wc_\theta & -s_\theta c_w \\ c_{331}c_W & -(c_{331}s_Wc_\theta + s_{331}s_\theta) & (c_{331}s_Ws_\theta - s_{331}c_\theta) \end{pmatrix}.$$

Next, the gauge bosons are defined such as $Z_1 \equiv Z$ and $Z_2 \equiv Z'$, where Z is the boson found experimentally.

The model includes five CP - odd neutral scalar components contained in the five neutral Higgs boson $\eta_1^0 = (v_2 + R_1 + iI_1)/\sqrt{2}$, $\rho^0 = (v_1 + R_2 + iI_2)/\sqrt{2}$, $\chi_2^0 = (\omega + R_3 + iI_3)/\sqrt{2}$, $\eta_2^0 = (R_4 + iI_4)/\sqrt{2}$, and $\chi_1^0 = (R_5 + iI_5)/\sqrt{2}$. Which have three Goldstone bosons of the neutral gauge bosons as Z, Z' , and X^0 . Others are physical states with masses

$$m_{a_1}^2 = (s_\beta^2 v^2 + \omega^2) \left(ft_\beta^{-1} + \frac{1}{2}\tilde{\lambda}_{13} \right), \quad m_{a_2}^2 = f \left(\frac{\omega^2}{c_\beta s_\beta} + c_\beta s_\beta v^2 \right). \quad (27)$$

Consequently, $f > 0$ condition are required for the term f .

Examining the CP-even scalars, in two bases (η_2^0, χ_1^0) and $(\eta_1^0, \rho_1^0, \chi_1^0)$ are corresponding to two sub-matrices 2×2 and 3×3 for masses of these Higgs boson, detailed

$$M_{0,3}^2 = \begin{pmatrix} \frac{c_\beta f \omega^2}{s_\beta} + 2s_\beta^2 \lambda_1 v^2 & c_\beta s_\beta \lambda_{12} v^2 - \omega^2 f & \omega(s_\beta \lambda_{13} - c_\beta f)v \\ c_\beta s_\beta \lambda_{12} v^2 - \omega^2 f & \frac{s_\beta f \omega^2}{c_\beta} + 2v^2 c_\beta^2 \lambda_2 & v\omega(c_\beta \lambda_{23} - s_\beta f) \\ v\omega(s_\beta \lambda_{13} - c_\beta f) & v\omega(c_\beta \lambda_{23} - s_\beta f) & 2\lambda_3 \omega^2 + c_\beta s_\beta f v^2 \end{pmatrix},$$

$$M_{0,2}^2 = \begin{pmatrix} \frac{1}{2}\omega^2 \left(\tilde{\lambda}_{13} + \frac{2c_\beta f}{s_\beta} \right) & \frac{1}{2}v\omega(\tilde{\lambda}_{13}s_\beta + 2c_\beta f) \\ \frac{1}{2}v\omega(\tilde{\lambda}_{13}s_\beta + 2c_\beta f) & \frac{1}{2}v^2 s_\beta(\tilde{\lambda}_{13}s_\beta + 2c_\beta f) \end{pmatrix}. \quad (28)$$

The matrix $M_{0,2}^2$ has one zero value and $m_{h_4}^2 = \left(\frac{f}{t_\beta} + \frac{\tilde{\lambda}_{13}}{2} \right) (s_\beta^2 v^2 + \omega^2)$ consistent with the Goldstone boson of X^0 and the Higgs boson h_4^0 (heavy neutral boson) with mass at the $SU(3)_L$ breaking scale. Furthermore, research also shows that $\text{Det}[M_{0,3}^2]|_{v=0} = 0$, but $\text{Det}[M_{0,3}^2] \neq 0$. This implies that the electroweak scale needs to exist of at least one Higgs boson mass, which can be associated with the SM-like Higgs boson. Namely, it can be demonstrated that

$$C_1^h M_{0,3}^2 C_1^{hT}|_{v=0} = \text{diag} \left(0, 2\lambda_3 w^2, f\omega^2/(s_\beta c_\beta) \right), \quad C_1^h = \begin{pmatrix} s_\beta & c_\beta & 0 \\ -c_\beta & s_\beta & 0 \\ 0 & 0 & 1 \end{pmatrix}, \quad (29)$$

and $C_1^h M_{0,3}^2 C_1^{hT} \equiv M_{0,3}'^2$ satisfying

$$\begin{aligned} (M_{0,3}'^2)_{11} &= 2v^2 (c_\beta^4 \lambda_2 + c_\beta^2 \lambda_{12} s_\beta^2 + \lambda_1 s_\beta^4), \\ (M_{0,3}'^2)_{22} &= 2v^2 s_\beta^2 c_\beta^2 (\lambda_1 - \lambda_{12} + \lambda_2) + \frac{f\omega^2}{c_\beta s_\beta}, \\ (M_{0,3}'^2)_{33} &= f v^2 s_\beta c_\beta + 2\lambda_3 \omega^2, \\ (M_{0,3}'^2)_{12} &= (M_{0,3}'^2)_{21} = v^2 s_\beta c_\beta (s_\beta^2 (\lambda_{12} - 2\lambda_1) - c_\beta^2 (\lambda_{12} - 2\lambda_2)), \\ (M_{0,3}'^2)_{13} &= (M_{0,3}'^2)_{31} = v\omega (-2f s_\beta c_\beta + c_\beta^2 \lambda_{23} + \lambda_{13} s_\beta^2), \\ (M_{0,3}'^2)_{32} &= (M_{0,3}'^2)_{23} = v\omega (f c_\beta^2 - f s_\beta^2 + s_\beta c_\beta (\lambda_{23} - \lambda_{13})). \end{aligned} \quad (30)$$

As a result, by using unitary transformation C_2^h with $(C_2^h)_{ij} \sim \mathcal{O}(v/w)$ ($i \neq j$) so that $C_2^h M_{0,3}'^2 C_2^{hT} = \text{diag} (m_{h_1^0}^2, m_{h_2^0}^2, m_{h_3^0}^2)$ and $m_{h_1^0}^2 \sim \mathcal{O}(v^2)$ [15]. Hence $h_1^0 \equiv h$ is determined with the SM-like Higgs boson found by experiment at the LHC, where only $\text{Re}[\eta_1^0] = R_1/\sqrt{2}$ and $\text{Re}[\rho_1^0] \sim / \sqrt{2}$ give contributions to h_1^0 , particular

$$R_1 = s_\beta \times h_1^0 - c_\beta \times h_2^0, \quad R_2 = c_\beta \times h_1^0 + s_\beta \times h_2^0. \quad (31)$$

Based on the presented result, the couplings and their one-loop contributions of decays above mentioned all will be derived and are shown in detail in the next section.

III. COUPLINGS AND ANALYTIC FORMULAS

A. Decays $Z \rightarrow e_a e_b$

The effective amplitude for the decays $Z \rightarrow e_a^\pm(p_1)e_b^\mp(p_2)$ is [6, 21]

$$i\mathcal{M}(Z \rightarrow e_b^+ e_a^-) = \frac{ie}{16\pi^2} \bar{u}_a [\not{\epsilon} (\bar{a}_l P_L + \bar{a}_r P_R) + (p_1 \cdot \epsilon) (\bar{b}_l P_L + \bar{b}_r P_R)] v_b, \quad (32)$$

where $\epsilon_\alpha(q)$, $u_a(p_1)$, and $v_b(p_2)$ are the polarization of Z and two Dirac spinors, respectively. By using the equation $q \cdot \epsilon = 0$, easily to see that $p_2 \cdot \epsilon = -p_1 \cdot \epsilon$, therefore simplify the representation shown in Ref. [6]. The correlating partial decay width is

$$\Gamma(Z \rightarrow e_b^+ e_a^-) = \frac{\sqrt{\lambda}}{16\pi m_Z^3} \times \left(\frac{e}{16\pi^2} \right)^2 \left(\frac{\lambda M_0}{12m_Z^2} + M_1 + \frac{\lambda M_2}{3m_Z^2} \right), \quad (33)$$

where $\lambda = m_Z^4 + m_b^4 + m_a^4 - 2(m_Z^2 m_a^2 + m_Z^2 m_b^2 + m_a^2 m_b^2) \simeq m_Z^4$ because of $m_a^2, m_b^2 \ll m_Z^2$, and

$$\begin{aligned} M_0 &= (m_Z^2 - m_a^2 - m_b^2) (|\bar{b}_l|^2 + |\bar{b}_r|^2) - 4m_a m_b \text{Re} [\bar{b}_l \bar{b}_r^*] \\ &\quad - 4m_b \text{Re} [\bar{a}_r^* \bar{b}_l^* + \bar{a}_l^* \bar{b}_r^*] - 4m_a \text{Re} [\bar{a}_l^* \bar{b}_l^* + \bar{a}_r^* \bar{b}_r^*], \\ M_1 &= 4m_a m_b \text{Re} [\bar{a}_l \bar{a}_r^*], \\ M_2 &= \left[2m_Z^4 - m_Z^2 (m_a^2 + m_b^2) - (m_a^2 - m_b^2)^2 \right] (|\bar{a}_l|^2 + |\bar{a}_r|^2). \end{aligned} \quad (34)$$

The relevant one-loop diagrams contributing to the decay amplitude $Z \rightarrow e_a e_b$ in the unitary gauge are illustrated in Fig. 1. The couplings of charged gauge bosons giving one-loop

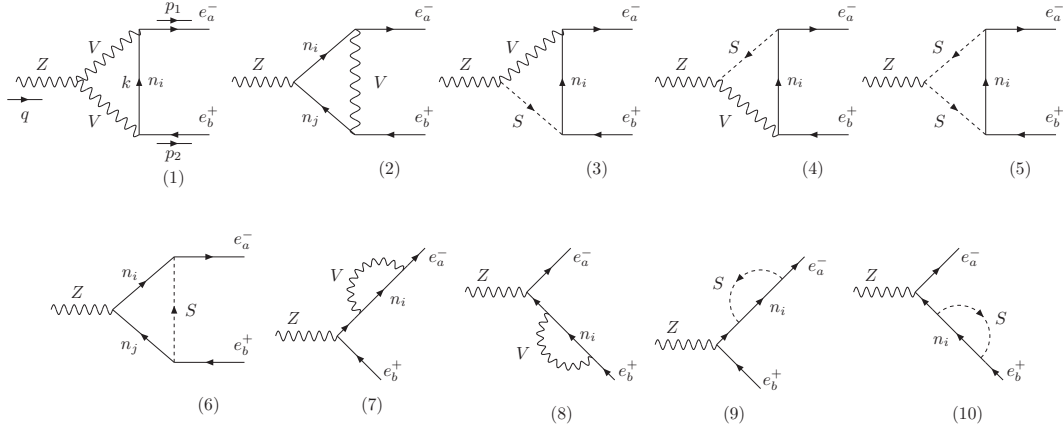


FIG. 1: One-loop Feynman diagrams contributing to $Z \rightarrow e_a e_b$ in the unitary gauge [6]

contributions to LFVZ amplitudes are

$$\mathcal{L}_{\text{Vff}}^Y = \frac{g}{\sqrt{2}} \sum_{a=1}^3 \sum_{i=1}^9 \bar{n}_i \gamma^\mu P_L e_a [U_{ai}^{\nu*} W_\mu^+ + U_{(a+3)i}^{\nu*} Y_\mu^+] + h.c., \quad (35)$$

Vertex	Coupling
$W_\mu^+ \bar{n}_i e_b, W_\mu^- \bar{e}_a n_i,$	$\frac{ig}{\sqrt{2}} U_{ai}^{\nu*} \gamma^\mu P_L, \frac{ig}{\sqrt{2}} U_{ai}^\nu \gamma^\mu P_L$
$Y_\mu^+ \bar{n}_i e_b, Y_\mu^- \bar{e}_a n_i$	$\frac{ig}{\sqrt{2}} U_{(a+3)i}^{\nu*} \gamma^\mu P_L, \frac{ig}{\sqrt{2}} U_{(a+3)i}^\nu \gamma^\mu P_L$

TABLE I: Feynman rules relevant one-loop contributions to $Z \rightarrow e_a e_b$ in the unitary gauge relate between gauge boson and two different leptons.

The couplings between three gauge bosons originate from the covariant kinetic Lagrangian of the non-Abelian gauge bosons:

$$\mathcal{L}_D^g = -\frac{1}{4} \sum_{a=1}^8 F_{\mu\nu}^a F^{a\mu\nu}, \quad (36)$$

where

$$F_{\mu\nu}^a = \partial_\mu W_\nu^a - \partial_\nu W_\mu^a + g \sum_{b,c=1}^8 f^{abc} W_\mu^b W_\nu^c, \quad (37)$$

where f^{abc} ($a, b, c = 1, 2, \dots, 8$) are structure constants of the $SU(3)$ group, which identified as

$$\begin{aligned} \mathcal{L}_D^g = & - \sum_{V=W,Y} eg_{ZVV} Z^\mu(p_0) V^{+\nu}(p_+) V^{-\lambda}(p_-) \times \Gamma_{\mu\nu\lambda}(p_0, p_+, p_-), \\ & - e \sum_{V=W,Y} A^\mu(p_0) V^{+\nu}(p_+) V^{-\lambda}(p_-) \times \Gamma_{\mu\nu\lambda}(p_0, p_+, p_-) + \dots, \end{aligned} \quad (38)$$

where $\Gamma_{\alpha\beta\sigma}(p_0, p_+, p_-) \equiv g_{\alpha\beta}(p_0 - p_+)_\sigma + g_{\beta\sigma}(p_+ - p_-)_\alpha + g_{\sigma\alpha}(p_- - p_0)_\beta$, and $V = W^\pm, Y^\pm$.

In table II show the involving couplings of Z .

Vertex	Coupling
g_{ZW+W^-}	$t_W^{-1} c_\theta$
g_{ZY+Y^-}	$\frac{1}{2s_W} \left[c_\theta c_W (1 - t_W^2) + s_\theta \sqrt{3 - t_W^2} \right]$

TABLE II: Feynman rules for triple gauge couplings corresponding with LFVZ decays.

The covariant kinetic terms of the Higgs bosons include the couplings of Higgs and gauge bosons are presented

$$\mathcal{L}_{\text{kin}}^\phi = \sum_{\phi=\chi,\rho,\eta} (D_\mu \phi)^\dagger (D^\mu \phi)$$

$$\begin{aligned}
&= g_{hWW} g_{\mu\nu} h W^{-\mu} W^{+\nu} + g_{hYY} g_{\mu\nu} h Y^{-\mu} Y^{+\nu} \\
&+ \left[-ig_{hh_1^\pm W}^* (h_1^+ \partial_\mu h - h \partial_\mu h_1^+) W^{-\mu} + ig_{hh_1^\pm W} (h_1^- \partial_\mu h - h \partial_\mu h_1^-) W^{+\mu} \right] \\
&+ \left[-ig_{hh_2^\pm Y}^* (h_2^+ \partial_\mu h - h \partial_\mu h_2^+) Y^{-\mu} + ig_{hh_2^\pm Y} (h_2^- \partial_\mu h - h \partial_\mu h_2^-) Y^{+\mu} \right] \\
&+ \sum_{k=1}^2 ieA^\mu (h_k^- \partial_\mu h_k^+ - h_k^+ \partial_\mu h_k^-) + \sum_{k=1}^2 ieg_{Zh_k^+ h_k^-} Z^\mu (h_k^- \partial_\mu h_k^+ - h_k^+ \partial_\mu h_k^-) \\
&+ Z^\mu e \left[ig_{ZW+h_1^-} W^{+\nu} h_1^- g_{\mu\nu} + ig_{ZW+h_1^-}^* W^{-\nu} h_1^+ g_{\mu\nu} \right] \\
&+ Z^\mu e \left[ig_{ZY+h_2^-} Y^{+\nu} h_2^- g_{\mu\nu} + ig_{ZY+h_2^-}^* Y^{-\nu} h_2^+ g_{\mu\nu} \right] + \dots \tag{39}
\end{aligned}$$

Then, we present the corresponding terms contributing to the decays $Z \rightarrow e_a e_b$ from the second line in Eq. (39). In the Table III show the relevant Feynman rules, where $\partial_\mu h \rightarrow -ip_{0\mu} h$ and $\partial_\mu h_i^\pm \rightarrow -ip_{\pm\mu} h_i^\pm$, leading to $i(h_i^- \partial_\mu h_i^+ - h_i^+ \partial_\mu h_i^-) = h_i^- h_i^+ (p_+ - p_-)_\mu$. The incoming momenta are denoted p_0, p_\pm .

Vertex	Coupling	
$g_{Zh_1^+ h_1^-}$	$\frac{1}{2c_W s_W}$	$c_\theta (1 - 2s_W^2) + \frac{c_W s_\theta (2\sqrt{3}c_\beta^2 - \frac{1}{\sqrt{3}}t_W^2 - \sqrt{3})}{3\sqrt{1 - \frac{1}{3}t_W^2}}$
$g_{Zh_2^+ h_2^-}$	$\frac{1}{2s_W c_W}$	$c_\theta (s_{13}^2 - 2s_W^2) - \frac{s_\theta (c_{13}^2 - 2)(2s_W^2 - 1)}{\sqrt{3 - 4s_W^2}}$
$g_{ZW+h_1^-}$	$-\frac{s_\theta s_{2\beta} m_W}{t_W \sqrt{3 - 4s_W^2}}$	
$g_{ZY+h_2^-}$	$-\frac{c_\beta c_{13} m_W}{c_W s_W}$	$c_\theta + \frac{s_\theta (-1 + 2s_W^2)}{\sqrt{3 - 4s_W^2}}$

TABLE III: Feynman rules of couplings with Z to charged Higgs and gauge bosons.

The Lagrangian with Z couplings to leptons are

$$\begin{aligned}
L_{Z\ell\ell} = & e \left(c_\theta + \frac{s_\theta}{\sqrt{3 - 4s_W^2}} \right) \bar{e}_a \gamma^\mu \left[\frac{1}{s_W c_W} \left(-\frac{1}{2} + s_W^2 \right) P_L + t_W P_R \right] e_a Z_{1\mu} \\
& + \frac{ec_\theta}{2c_W s_W} \left[\left(1 + \frac{t_\theta (2s_W^2 - 1)}{\sqrt{3 - 4s_W^2}} \right) \bar{\nu}_a \gamma^\mu P_L \nu_a + \frac{4t_\theta c_W^2}{\sqrt{3 - 4s_W^2}} \bar{N}_a \gamma^\mu P_L N_a \right] Z_{1\mu}. \tag{40}
\end{aligned}$$

Return according to Feynman rules of couplings with Z to two Majorana leptons n_i and n_j by using the form:

$$\begin{aligned}
\mathcal{L}_{Z\ell\ell} = & \sum_{i,j=1}^9 \left[\frac{e}{2} \bar{n}_i \gamma^\mu (G_{ij} P_L - G_{ji} P_R) n_j Z_\mu \right], \\
G_{ij} = & \frac{c_\theta}{2c_W s_W} \sum_{c=1}^3 \left[\left(1 + \frac{t_\theta (2s_W^2 - 1)}{\sqrt{3 - 4s_W^2}} \right) U_{ci}^{\nu*} U_{cj}^\nu + \frac{4t_\theta c_W^2}{\sqrt{3 - 4s_W^2}} U_{(c+3)i}^{\nu*} U_{(c+3)j}^\nu \right]. \tag{41}
\end{aligned}$$

Therefore, we consider the limit $\theta = 0$, leading to the same coupling of Z given in Ref. [1], consistent with 2HDM results.

$$\mathcal{L}_{\text{int}} = \sum_{i,j=1}^9 \left[-\frac{g}{4m_W} \bar{n}_i (\lambda_{ij}^h P_L + \lambda_{ij}^{h*} P_R) n_j h + \frac{e}{2} \bar{n}_i \gamma^\mu (G_{ij} P_L - G_{ji} P_R) n_j Z_\mu \right], \quad (42)$$

where

$$\lambda_{ij}^h = \lambda_{ji}^h = \sum_{c=1}^3 (U_{ci}^{\nu*} m_{n_i} U_{cj}^\nu + U_{cj}^{\nu*} m_{n_j} U_{ci}^\nu). \quad (43)$$

Following with Ref. [2], the Yukawa couplings of leptons with charged Higgs boson are identified as

$$\mathcal{L}^{\ell n h^\pm} = -\frac{g}{\sqrt{2}m_W} \sum_{k=1}^2 \sum_{a=1}^3 \sum_{i=1}^9 h_k^\pm \bar{n}_i \left(\lambda_{ai}^{L,k} P_L + \lambda_{ai}^{R,k} P_R \right) e_a + \text{h.c.}, \quad (44)$$

we defined

$$\begin{aligned} \lambda_{ai}^{R,1} &= m_a t_\beta U_{ai}^{\nu*}, & \lambda_{ai}^{L,1} &= s_\beta z_0 e^{i\alpha_{23}} \sum_{c=1}^3 (\tilde{m}_D)_{ac} U_{(c+3)i}^\nu, \\ \lambda_{ai}^{R,2} &= \frac{m_a c_\theta U_{(a+3)i}^{\nu*}}{c_\beta}, & \lambda_{ai}^{L,2} &= c_\theta z_0 \sum_{c=1}^3 \left[-e^{i\alpha_{23}} (\tilde{m}_D)_{ac} U_{ci}^\nu + t_\theta^2 (\tilde{M}_R^T)_{ac} U_{(c+6)i}^\nu \right]. \end{aligned} \quad (45)$$

B. Decays $h \rightarrow e_a e_b$

One-loop contributions of this LFV h decays were introduced previously, see Ref. [2], which will be used to investigate simultaneously with LFV Z and cLFV decays in this work. We will use the analytical formulas given in Ref. [2].

IV. NUMERICAL DISCUSSION

In this paper, we will investigate the neutrino oscillation data given in Refs. [23, 24]. The lepton mixing matrix U_{PMNS} have the standard form is the function of follow angles θ_{ij} , one Dirac phase δ and two Majorana phases α_1 and α_2 [25], in particular

$$\begin{aligned} U_{\text{PMNS}}^{\text{PDG}} &= f(\theta_{12}, \theta_{13}, \theta_{23}, \delta) \times \text{diag}(1, e^{i\alpha_1}, e^{i\alpha_2}), \\ f(\theta_{12}, \theta_{13}, \theta_{23}, \delta) &\equiv \begin{pmatrix} 1 & 0 & 0 \\ 0 & c_{23} & s_{23} \\ 0 & -s_{23} & c_{23} \end{pmatrix} \begin{pmatrix} c_{13} & 0 & s_{13} e^{-i\delta} \\ 0 & 1 & 0 \\ -s_{13} e^{i\delta} & 0 & c_{13} \end{pmatrix} \begin{pmatrix} c_{12} & s_{12} & 0 \\ -s_{12} & c_{12} & 0 \\ 0 & 0 & 1 \end{pmatrix}, \end{aligned} \quad (46)$$

where $c_{ij} \equiv \cos \theta_{ij}$, $s_{ij} \equiv \sin \theta_{ij}$, $i, j = 1, 2, 3$ ($i < j$), $0 \leq \theta_{ij} < 90$ [Deg.] and $0 < \delta \leq 720$ [Deg.]. We fix the range $-180 \leq \alpha_i \leq 180$ [Deg.] for the Majorana phases. For numerical research, benchmark relating to the NO (normal order) of the neutrino oscillation data [26] will be selected as the input to fix \tilde{m}_D that $s_{12}^2 = 0.32$, $s_{13}^2 = 0.0216$, $s_{23}^2 = 0.547$, $\Delta m_{32}^2 = 2.424 \times 10^{-3}[\text{eV}^2]$, $\Delta m_{21}^2 = 7.55 \times 10^{-5}[\text{eV}^2]$, $\delta = 180$ [Deg], and $\alpha_1 = \alpha_2 = 0$. As consequence, the matrix \tilde{m}_D which the reduced Dirac mass matrix is chosen below

$$\tilde{m}_D = \begin{pmatrix} 0 & 0.613 & 0.357 \\ -0.613 & 0 & 1 \\ -0.357 & -1 & 0 \end{pmatrix}. \quad (47)$$

The mixing matrix V_R is parameterized in the similar as $V_R = f(\theta_{12}^r, \theta_{13}^r, \theta_{23}^r, 0)$, where the scanning ranges for the angles $\theta_{ij}^r \in [0, 2\pi]$. The remaining free terms are explored within the following ranges:

$$\begin{aligned} \hat{k}_{1,2,3} &\geq 5, \quad 1 \text{ [TeV]} \leq m_{h_1^\pm}, m_{h_2^\pm} \leq 5 \text{ [TeV]}, \\ t_\beta &\in [0.5, 40], \quad 100 \text{ [GeV]} \leq z \leq 600 \text{ [GeV]}. \end{aligned} \quad (48)$$

$G_F = 1.663787 \times 10^{-5} \text{ [GeV}^{-2}]$, $\alpha_{em} = e^2/(4\pi) = 1/137$, $g = 0.652$, $s_W^2 = 0.231$, $m_e = 5.0 \times 10^{-4} \text{ [GeV]}$, $m_\mu = 0.105 \text{ [GeV]}$, $m_\tau = 1.776 \text{ [GeV]}$, $m_Z = 91.1876 \text{ [GeV]}$, and $m_W = 80.385 \text{ [GeV]}$, and the total decay width of the Z boson is $\Gamma_Z = 2.4955 \text{ GeV}$ are the parameters which are found in experiment. The well-known decays used in this research are $\text{Br}(\mu \rightarrow e \bar{\nu}_e \nu_\mu) \simeq 1$, $\text{Br}(\tau \rightarrow \mu \bar{\nu}_\mu \nu_\tau) \simeq 0.1739$, and $\text{Br}(\tau \rightarrow e \bar{\nu}_e \nu_\tau) \simeq 0.1782$ [26].

The dependence of LFV decays on z_0 from numerical results are presented in Fig. 2. According to illustrated in Fig 2, we can see that LFVZ decay rates depend strongly on z_0 ,

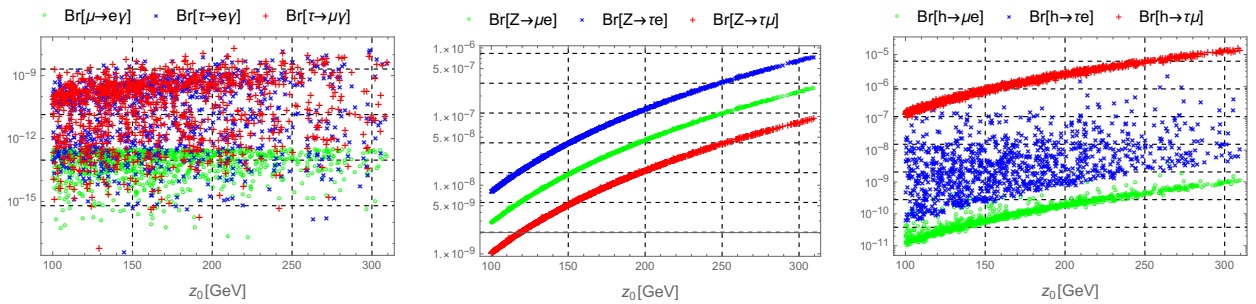


FIG. 2: The dependence of LFV decays rate on z_0 .

which are given in three narrow curves in the middle panel of Fig. 2. Additionally, we have

an interesting consequence that the upper constraint of $\text{Br}(Z \rightarrow \mu^+e^-) \leq 2.62 \times 10^{-7}$ gives the most strict upper bound on z_0 , namely $z_0 \leq 310$ GeV. Similarly, for the two LFV h decays $h \rightarrow \mu e, \tau\mu$, which have upper bounds of $\text{Br}(h \rightarrow \mu e) < 10^{-8}$, and $\text{Br}(h \rightarrow \tau\mu) < 5 \times 10^{-5}$, resulting from $z_0 \leq 310$ GeV. Therefore, if one of these five decay rates are detected, the remaining values can be predicted precisely.

The dependence of LFV decays on t_β is shown in Fig. 3. Corresponding to the chosen

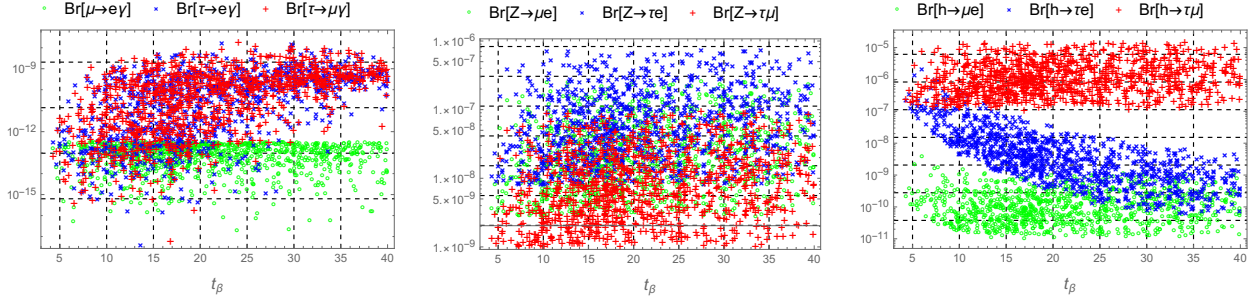


FIG. 3: The dependence of LFV decay rates on t_β .

scanning range of the parameter t_β given in Eq. (48), we see that all $\text{Br}(\text{LFV})$ depend on t_β and the upper bounds are consistent with the constraints from current experiments as [27–30] $\text{Br}(\mu \rightarrow e\gamma) < 3.1 \times 10^{-13}$, $\text{Br}(\tau \rightarrow \mu\gamma) < 4.2 \times 10^{-8}$, $\text{Br}(\tau \rightarrow e\gamma) < 3.3 \times 10^{-8}$. They will not be excluded by the future sensitivity as follows [31, 32]: $\text{Br}(\mu \rightarrow e\gamma) < 6 \times 10^{-14}$, $\text{Br}(\tau \rightarrow \mu\gamma) < 6.9 \times 10^{-9}$, $\text{Br}(\tau \rightarrow e\gamma) < 9 \times 10^{-9}$. Next, the upper bound of LFV Z decays are $\max[\text{Br}(Z \rightarrow \mu e)] \simeq 2.4 \times 10^{-7}$, $\max[\text{Br}(Z \rightarrow \tau\mu)] \simeq 1. \times 10^{-7}$, and $\max[\text{Br}(Z \rightarrow \tau e)] \simeq 8.8 \times 10^{-7}$. We can see, only the decay rate ($Z \rightarrow \mu e$) is close to the latest experimental bound, $\text{Br}(Z \rightarrow \mu e) < 2.62 \times 10^{-7}$ [12], but the two other decay modes are still much smaller than that of the recent experimental sensitivities as [11] $\text{Br}(Z \rightarrow \tau e) \simeq 5.0 \times 10^{-6}$ and $\text{Br}(Z \rightarrow \tau\mu) \simeq 6.5 \times 10^{-6}$. However, the future sensitivities for these decays at HL-LHC [13] will be 10^{-6} , 10^{-6} and 10^{-7} ; and at FCC-ee [13, 14] will be 10^{-9} , 10^{-9} and 10^{-10} , respectively. The upper bounds of the LFV h decays are: $\text{Br}(h \rightarrow \mu e) < 10^{-8}$, $\text{Br}(h \rightarrow \tau e) < 5 \times 10^{-6}$, and $\text{Br}(h \rightarrow \tau\mu) < 5 \times 10^{-5}$. It is easy to see that, only $\text{Br}(h \rightarrow \tau\mu)$ possibly reach a significant value of the near future experimental sensitivities at the HL-LHC and e^+e^- colliders [33–35].

The correlations between LFV decays with $\text{Br}(\mu \rightarrow e\gamma)$, see illustrations in Fig. 4. We choose a survey value of $\text{Br}(\mu \rightarrow e\gamma)$ that satisfies the experimental limits: $\text{Br}(\mu \rightarrow e\gamma) \simeq 3.1 \times 10^{-13}$ as in Ref. [28]. Satisfying the requirement of $\text{Br}(e_b \rightarrow e_a\gamma)$ is the most stringent requirement in experiments. Therefore, all investigations of decay processes should

satisfy this condition. It shows that a large value of $\text{Br}(\mu \rightarrow e\gamma)$ predicts a large value of $\text{Br}(Z \rightarrow \tau e)$, and $\text{Br}(h \rightarrow \tau\mu)$. The upper bound of these decays are: $\text{Br}(\tau \rightarrow e(\mu)\gamma) \sim 10^{-8}$, $\text{Br}(Z \rightarrow \mu e) \sim 5. \times 10^{-7}$, $\text{Br}(Z \rightarrow \tau e) \sim 10^{-6}$, $\text{Br}(Z \rightarrow \tau\mu) \sim 10^{-7}$, $\text{Br}(h \rightarrow \tau\mu) \sim 2. \times 10^{-5}$, $\text{Br}(h \rightarrow \tau e) \sim 10^{-6}$, and $\text{Br}(h \rightarrow \mu e) \sim 10^{-9}$. It says that our results include all decay rates that can reach the corresponding expected future sensitivities, except $\text{Br}(h \rightarrow \mu e)$ still smaller than future experimental sensitivities.

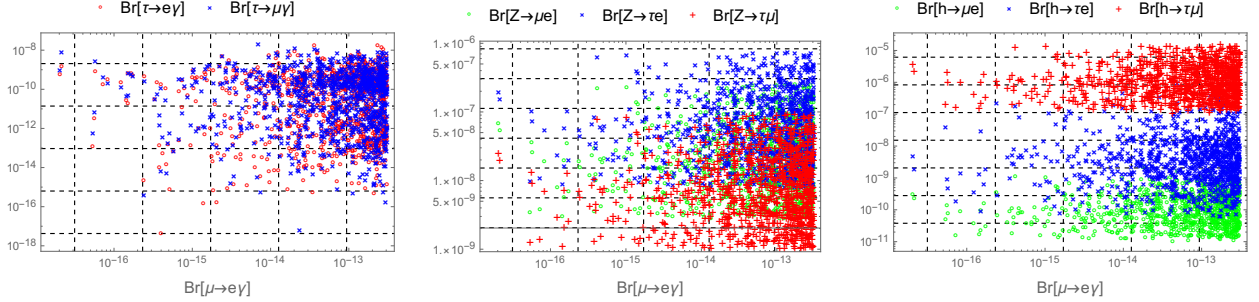


FIG. 4: The dependence of LFV decay rates on $\text{Br}(\mu \rightarrow e\gamma)$.

The correlations between LFV h and LFV Z decay rates are presented in Fig. 5. Over the value range of $\text{Br}(h \rightarrow e_a e_b)$ that satisfies experimental constraints, all Br of LFV Z decay channels depend strongly on these values as in Fig. 5. Particularly, the large value of $\text{Br}(h \rightarrow e_a e_b)$ predicts large value of $\text{Br}(Z \rightarrow e_a e_b)$, respectively. The upper bounds are nearly with with recent experiments.

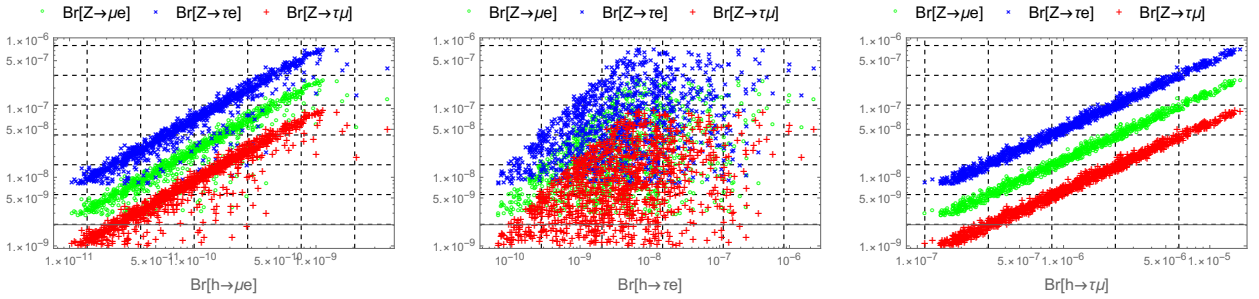


FIG. 5: The correlations between LFV h and LFV Z decay rates

V. CONCLUSION

In the 331 NL framework, we have studied in details the LFV decays, namely cLFV, LFV h and LFV Z . Here are the main results we obtained. Firstly, the numerical results showed

the strong dependence of LFVZ decay on z_0 . The numerical results showed that LFV decays dependence on t_β , only the decay rate ($Z \rightarrow \mu e$) is close to the latest experimental bound, and $\text{Br}(h \rightarrow \tau\mu)$ can reach the near future experimental sensitivities. Secondly, our results also make clear that the value of $\text{Br}(\mu \rightarrow e\gamma)$ proportional the value of $\text{Br}(Z \rightarrow \tau e)$ and $\text{Br}(h \rightarrow \tau\mu)$. Our results consist of all decay rates that can reach the corresponding expected future sensitivities, except $\text{Br}(h \rightarrow \mu e)$. Lastly, this research also gives the large value of $\text{Br}(h \rightarrow e_a e_b)$ predicts the large value of $\text{Br}(Z \rightarrow e_a e_b)$. The upper bounds of $\text{Br}(Z \rightarrow e_a e_b)$ also coincide with recent experiments. We stress that these results are similar to the results of previous research [5]. Besides that, in our studies, many LFV processes such as $h \rightarrow e_a e_b$, $e_b \rightarrow e_a \gamma$, and $Z \rightarrow e_a e_b$ discussed simultaneously. Therefore, survey results are more reliable and our work helps limit the region of the parameter space that can be effectively probed by forthcoming experiments in LFVZ decays.

Acknowledgments

We thank Dr. Le Tho Hue for useful comments.

Appendix A: One-loop form factors for LFVZ decays the unitary gauge

The form factors are calculated in the unitary gauge as in Ref. [1] as below. Diagram (1) in Fig 1 give one-loop contributions:

$$\begin{aligned} \bar{a}_l^{nGG} = \sum_{i=1}^9 g_{ab}^{LL} g_{ZGG} \left\{ \left[-4 + \frac{m_{n_i}^2}{m_G^2} \left(\frac{m_Z^2}{m_G^2} - 2 \right) \right] C_{00} + 2 (m_Z^2 - m_a^2 - m_b^2) X_3 \right. \\ \left. - \frac{1}{m_G^2} \left[m_Z^2 (2m_{n_i}^2 C_0 + m_a^2 C_1 + m_b^2 C_2) \right. \right. \\ \left. \left. - m_{n_i}^2 (B_0^{(1)} + B_0^{(2)}) - m_a^2 B_1^{(1)} - m_b^2 B_1^{(2)} \right] \right\}, \quad (\text{A1}) \end{aligned}$$

$$\bar{a}_r^{nGG} = \sum_{i=1}^9 g_{ab}^{LL} g_{ZGG} m_a m_b \left[\left(-4 + \frac{m_Z^2}{m_G^2} \right) X_3 + \frac{m_Z^2 - 2m_G^2}{m_G^4} C_{00} \right], \quad (\text{A2})$$

$$\bar{b}_l^{nGG} = \sum_{i=1}^9 g_{ab}^{LL} g_{ZGG} m_a \left[4 (X_3 - X_1) + \frac{m_Z^2 - 2m_G^2}{m_G^4} (m_{n_i}^2 X_{01} + m_b^2 X_2) - \frac{2m_Z^2}{m_G^2} C_2 \right], \quad (\text{A3})$$

$$\bar{b}_r^{nGG} = \sum_{i=1}^9 g_{ab}^{LL} g_{ZGG} m_b \left[4 (X_3 - X_2) + \frac{m_Z^2 - 2m_G^2}{m_G^4} (m_{n_i}^2 X_{02} + m_a^2 X_1) - \frac{2m_Z^2}{m_G^2} C_1 \right], \quad (\text{A4})$$

where $g_{ab}^{LL} \equiv g_{aiG}^{L*} g_{biG}^L$, the PV-functions $B_{0,1}^{(k)} = B_{0,1}^{(k)}(p_k^2; m_{n_i}^2, m_G^2)$, $C_{00,0,k,kl} = C_{00,0,k,kl}(m_a^2, m_Z^2, m_b^2; m_{n_i}^2, m_G^2, m_G^2)$, and $X_{0,k,kl}$ are identified in terms of the PV-functions for all $k, l = 1, 2$.

One-loop form factors from diagram (2) in Fig. 1 are:

$$\begin{aligned} \bar{a}_l^{Gnn} = \sum_{i,j=1}^9 \frac{g_{ab}^{LL}}{m_G^2} \left\{ G_{ij} \left[m_G^2 \left(4C_{00} + 2m_a^2 X_{01} + 2m_b^2 X_{02} - 2m_Z^2 (C_{12} + X_0) \right) \right. \right. \\ \left. \left. - (m_{n_i}^2 - m_a^2) B_0^{(1)} - (m_{n_j}^2 - m_b^2) B_0^{(2)} + m_a^2 B_1^{(1)} + m_b^2 B_1^{(2)} \right. \right. \\ \left. \left. + (m_{n_j}^2 m_a^2 + m_{n_i}^2 m_b^2 - m_a^2 m_b^2) X_0 - m_{n_i}^2 m_{n_j}^2 C_0 \right. \right. \\ \left. \left. - m_{n_i}^2 m_b^2 C_1 - m_{n_j}^2 m_a^2 C_2 \right] \right. \\ \left. + G_{ji} m_{n_i} m_{n_j} \left[2m_G^2 C_0 - 2C_{00} - m_a^2 C_{11} - m_b^2 C_{22} \right. \right. \\ \left. \left. + (m_Z^2 - m_a^2 - m_b^2) C_{12} \right] \right\}, \end{aligned} \quad (\text{A5})$$

$$\bar{a}_r^{Gnn} = \sum_{i,j=1}^9 \frac{g_{ab}^{LL}}{m_G^2} m_a m_b G_{ij} \left[2C_{00} + 2m_G^2 X_0 + m_a^2 X_1 + m_b^2 X_2 - m_Z^2 C_{12} - m_{n_i}^2 C_1 - m_{n_j}^2 C_2 \right], \quad (\text{A6})$$

$$\bar{b}_l^{Gnn} = \sum_{i,j=1}^9 \frac{g_{ab}^{LL}}{m_G^2} m_a \left[G_{ij} \left(-2m_G^2 X_{01} - m_b^2 X_2 + m_{n_j}^2 C_2 \right) + G_{ji} m_{n_i} m_{n_j} (X_1 - C_1) \right], \quad (\text{A7})$$

$$\bar{b}_r^{Gnn} = \sum_{i,j=1}^9 \frac{g_{ab}^{LL}}{m_G^2} m_b \left[G_{ij} \left(-2m_G^2 X_{02} - m_a^2 X_1 + m_{n_i}^2 C_1 \right) + G_{ji} m_{n_i} m_{n_j} (X_2 - C_2) \right], \quad (\text{A8})$$

where $g_{ab}^{LL} \equiv g_{aiG}^{L*} g_{bjG}^L$,

$$B_{0,1}^{(1)} = B_{0,1}^{(1)}(p_1^2; m_G^2, m_{n_i}^2), B_{0,1}^{(2)} = B_{0,1}^{(2)}(p_2^2; m_G^2, m_{n_j}^2),$$

and $C_{00,0,k,kl} = C_{00,0,k,kl}(m_a^2, m_Z^2, m_b^2; m_G^2, m_{n_i}^2, m_{n_j}^2)$ for $k, l = 1, 2$.

Two diagrams (7) and (8) in Fig. 1 give sum contributions that have form factors

$$\begin{aligned} \bar{a}_l^{nG} = \frac{g_{Ze}^L}{m_G^2 (m_a^2 - m_b^2)} \sum_{i=1}^9 g_{ab}^{LL} \left\{ 2m_{n_i}^2 (m_a^2 B_0^{(1)} - m_b^2 B_0^{(2)}) + m_a^4 B_1^{(1)} - m_b^4 B_1^{(2)} \right. \\ \left. + (2m_G^2 + m_{n_i}^2) \left(m_a^2 B_1^{(1)} - m_b^2 B_1^{(2)} \right) \right\}. \end{aligned} \quad (\text{A9})$$

$$\begin{aligned} \bar{a}_r^{nG} = \frac{m_a m_b g_{Ze}^R}{m_G^2 (m_a^2 - m_b^2)} \sum_{i=1}^9 g_{ab}^{LL} \left\{ 2m_{n_i}^2 (B_0^{(1)} - B_0^{(2)}) + m_a^2 B_1^{(1)} - m_b^2 B_1^{(2)} \right. \\ \left. + (2m_G^2 + m_{n_i}^2) \left(B_1^{(1)} - B_1^{(2)} \right) \right\}, \end{aligned} \quad (\text{A10})$$

$$\bar{b}_l^{nG} = \bar{b}_r^{nG} = 0, \quad (\text{A11})$$

where $g_{ab}^{XY} \equiv g_{aiG}^{X*} g_{biG}^Y$ with $X, Y = L, R$, and $B_{0,1}^{(k)} = B_{0,1}^{(k)}(p_k^2; m_{n_i}^2, m_G^2)$ with $k = 1, 2$.

In the limit $\theta = 0$, the contributions from W^\pm corresponding to diagrams (1), (2), (7), and (8) of Fig. 1 are:

$$m_G = m_W, \quad g_{ZGG} = g_{ZWW} = t_W^{-1}, \quad g_{aiG}^L = g_{aiW}^L = \frac{g}{\sqrt{2}} U_{ai}^{\nu*}, \quad (\text{A12})$$

and G_{ij} is given in Eq. (41).

The contributions from Y^\pm corresponding to diagrams (1), (2), (7), and (8) of Fig. 1 are:

$$m_G = m_Y, \quad g_{ZGG} = g_{ZYY} = \frac{1 - t_W^2}{t_W}, \quad g_{aiG}^L = g_{aiY}^L = \frac{g}{\sqrt{2}} U_{(a+3)i}^{\nu*}, \quad (\text{A13})$$

The two diagrams (3) and (4) appearing in the model under consideration were not discussed previously, we list here for completeness the form factors of diagram (3) in Fig. 1 are:

$$\begin{aligned} \bar{a}_l^{nGH} &= \sum_{i=1}^9 -\frac{g_{ZGH} g_{aiG}^{L*}}{m_G^2} [g_{biH}^L m_{n_i} (m_G^2 C_0 - C_{00}) - g_{biH}^R m_b m_G^2 C_2], \\ \bar{a}_r^{nGH} &= \sum_{i=1}^9 -\frac{g_{ZGH} g_{aiG}^{L*}}{m_G^2} \times g_{biH}^R m_a (C_{00} + m_G^2 C_1), \\ \bar{b}_l^{nGH} &= \sum_{i=1}^9 -\frac{g_{ZGH} g_{aiG}^{L*}}{m_G^2} [m_a (g_{biH}^R m_b X_2 - g_{biH}^L m_{n_i} X_{01})], \\ \bar{b}_r^{nGH} &= \sum_{i=1}^9 -\frac{g_{ZGH} g_{aiG}^{L*}}{m_G^2} [g_{biH}^R (m_{n_i}^2 X_0 + m_a^2 X_1 - 2m_G^2 C_1) - g_{biH}^L m_{n_i} m_b X_2]. \end{aligned} \quad (\text{A14})$$

The contributions of the two diagrams (3) and (4) are suppressed because of tiny mixing in $g_{ZW h_1}$ and large $m_G = m_Y \gg m_W$.

The form factors relating to diagram (4) are:

$$\begin{aligned} \bar{a}_l^{nHG} &= \sum_{i=1}^9 -\frac{g_{ZGH} g_{biG}^L}{m_G^2} [g_{aiH}^{L*} m_{n_i} (m_G^2 C_0 - C_{00}) - g_{aiH}^{R*} m_a m_G^2 C_1], \\ \bar{a}_r^{nHG} &= \sum_{i=1}^9 -\frac{g_{ZGH} g_{biG}^L}{m_G^2} [g_{aiH}^{R*} m_b (m_G^2 C_2 + C_{00})], \\ \bar{b}_l^{nHG} &= \sum_{i=1}^9 -\frac{g_{ZGH} g_{biG}^L}{m_G^2} [g_{aiH}^{R*} (m_{n_i}^2 X_0 + m_b^2 X_2 - 2m_G^2 C_2) - g_{aiH}^{L*} m_a m_{n_i} X_1], \\ \bar{b}_r^{nHG} &= \sum_{i=1}^9 -\frac{g_{ZGH} g_{biG}^L m_b}{m_G^2} [g_{aiH}^{R*} m_a X_1 - g_{aiH}^{L*} m_{n_i} X_{02}], \end{aligned} \quad (\text{A15})$$

In this models there are two classes of these contributions, namely:

$$m_G = m_W, \quad m_H = m_{h_1^\pm}, \quad g_{aiH}^L = -\frac{g\lambda_{ai}^{L,1}}{\sqrt{2}m_W}, \quad g_{ZGH} = g_{ZW+h_1^-} = -\frac{s_\theta s_{2\beta} m_W}{t_W \sqrt{3-4s_W^2}} \rightarrow 0, \quad (\text{A16})$$

and

$$m_G = m_Y, \quad m_H = m_{h_2^\pm}, \quad g_{aiH}^L = -\frac{g\lambda_{ai}^{L,2}}{\sqrt{2}m_W}, \quad g_{ZGH} = g_{ZY+h_2^-} = -\frac{c_\beta c_{13} m_W}{c_W s_W}. \quad (\text{A17})$$

The scalar exchanges are determined based on previous works [1, 5, 6] give one-loop contributions. Form factors corresponding to diagrams (5) are:

$$\begin{aligned} \bar{a}_l^{nss} &= -\frac{g^2}{m_W^2} \sum_{k=1}^2 \sum_{i=1}^9 g_{Zh_k^+ h_k^-} \lambda_{ai}^{L,k*} \lambda_{bi}^{L,k} C_{00}, \\ \bar{a}_r^{nss} &= -\frac{g^2}{m_W^2} \sum_{k=1}^2 \sum_{i=1}^9 g_{Zh_k^+ h_k^-} \lambda_{ai}^{R,k*} \lambda_{bi}^{R,k} C_{00}, \\ \bar{b}_l^{nss} &= -\frac{g^2}{m_W^2} \sum_{k=1}^2 \sum_{i=1}^9 g_{Zh_k^+ h_k^-} \left[m_a \lambda_{ai}^{L,k*} \lambda_{bi}^{L,k} X_1 + m_b \lambda_{ai}^{R,k*} \lambda_{bi}^{R,k} X_2 - m_{n_i} \lambda_{ai}^{R,k*} \lambda_{bi}^{L,k} X_0 \right], \\ \bar{b}_r^{nss} &= -\frac{g^2}{m_W^2} \sum_{k=1}^2 \sum_{i=1}^9 g_{Zh_k^+ h_k^-} \left[m_a \lambda_{ai}^{R,k*} \lambda_{bi}^{R,k} X_1 + m_b \lambda_{ai}^{L,k*} \lambda_{bi}^{L,k} X_2 - m_{n_i} \lambda_{ai}^{L,k*} \lambda_{bi}^{R,k} X_0 \right], \end{aligned} \quad (\text{A18})$$

where $g_{Zh^+kh^-}$ were given in Table III, and $\lambda_{ab}^{XY,k} \equiv \lambda_{ai}^{X,k*} \lambda_{bj}^{Y,k}$ with $X, Y = L, R$. The arguments for PV-functions are $(m_{n_i^2}, m_{h_k^\pm}^2, m_{h_k^\pm}^2)$.

The contributions from diagram (6) is

$$\begin{aligned} \bar{a}_l^{snn} &= -\frac{g^2}{2m_W^2} \sum_{k=1}^2 \sum_{i,j=1}^9 \left\{ G_{ij} \left[\lambda_{ab}^{LL,k} m_{n_i} m_{n_j} C_0 + \lambda_{ab}^{RL,k} m_a m_{n_j} (C_0 + C_1) \right. \right. \\ &\quad \left. \left. + \lambda_{ab}^{LR,k} m_b m_{n_i} (C_0 + C_2) + \lambda_{ab}^{RR,k} m_a m_b X_0 \right] \right. \\ &\quad \left. - G_{ji} \left[-\lambda_{ab}^{LL,k} (2C_{00} + m_a^2 X_1 + m_b^2 X_2 - m_Z^2 C_{12}) \right. \right. \\ &\quad \left. \left. - m_a m_{n_i} \lambda_{ab}^{RL,k} C_1 - m_b m_{n_j} \lambda_{ab}^{LR,k} C_2 \right] \right\} \\ \bar{a}_r^{snn} &= -\frac{g^2}{2m_W^2} \sum_{k=1}^2 \sum_{i,j=1}^9 \left\{ G_{ij} \left[-\lambda_{ab}^{RR,k} (2C_{00} + m_a^2 X_1 + m_b^2 X_2 - m_Z^2 C_{12}) \right. \right. \\ &\quad \left. \left. - \lambda_{ab}^{LR,k} m_a m_{n_i} C_1 - \lambda_{ab}^{RL,k} m_b m_{n_j} C_2 \right] \right. \\ &\quad \left. - G_{ji} \left[\lambda_{ab}^{RR,k} m_{n_i} m_{n_j} C_0 + \lambda_{ab}^{LR,k} m_a m_{n_j} (C_0 + C_1) \right. \right. \\ &\quad \left. \left. + \lambda_{ab}^{RL,k} m_b m_{n_i} (C_0 + C_2) + \lambda_{ab}^{LL,k} m_a m_b X_0 \right] \right\}, \end{aligned}$$

$$\begin{aligned}
\bar{b}_l^{snn} &= -\frac{g^2}{m_W^2} \sum_{k=1}^2 \sum_{i,j=1}^9 \left[G_{ij} \left(\lambda_{ab}^{RL,k} m_{n_j} C_2 + \lambda_{ab}^{RR,k} m_b X_2 \right) - G_{ji} \left(\lambda_{ab}^{RL,k} m_{n_i} C_1 + \lambda_{ab}^{LL,k} m_a X_1 \right) \right], \\
\bar{b}_r^{snn} &= -\frac{g^2}{m_W^2} \sum_{k=1}^2 \sum_{i,j=1}^9 \left[G_{ij} \left(\lambda_{ab}^{LR,k} m_{n_i} C_1 + \lambda_{ab}^{RR,k} m_a X_1 \right) - G_{ji} \left(\lambda_{ab}^{LR,k} m_{n_j} C_2 + \lambda_{ab}^{LL,k} m_b X_2 \right) \right],
\end{aligned} \tag{A19}$$

where $\lambda_{ab}^{XY,k} \equiv \lambda_{ai}^{X,k*} \lambda_{bj}^{Y,k}$ with $X, Y = L, R$. The PV-functions and their linear combinations are $F = F(m_a^2, m_Z^2, m_b^2; m_{h_k^\pm}^2, m_{n_i}^2, m_{n_j}^2)$ for all $F = C_{00,0,i,ij}, X_{0,i}$ with $i, j = 1, 2$.

Sum of two diagrams (9) and (10) gives the following non-zero contributions

$$\begin{aligned}
\bar{a}_l^{ns} &= -\frac{g^2 g_{Ze}^L}{2m_W^2 (m_a^2 - m_b^2)} \sum_{k=1}^2 \sum_{i=1}^9 \left[m_{n_i} \left(m_a \lambda_{ab}^{RL,k} + m_b \lambda_{ab}^{LR,k} \right) \left(B_0^{(1)} - B_0^{(2)} \right) \right. \\
&\quad \left. - m_a m_b \lambda_{ab}^{RR,k} \left(B_1^{(1)} - B_1^{(2)} \right) - \lambda_{ab}^{LL,k} \left(m_a^2 B_1^{(1)} - m_b^2 B_1^{(2)} \right) \right], \\
\bar{a}_r^{ns} &= -\frac{g^2 g_{Ze}^R}{2m_W^2 (m_a^2 - m_b^2)} \sum_{k=1}^2 \sum_{i=1}^9 \left[m_{n_i} \left(m_a \lambda_{ab}^{LR,k} + m_b \lambda_{ab}^{RL,k} \right) \left(B_0^{(1)} - B_0^{(2)} \right) \right. \\
&\quad \left. - m_a m_b \lambda_{ab}^{LL,k} \left(B_1^{(1)} - B_1^{(2)} \right) - \lambda_{ab}^{RR,k} \left(m_a^2 B_1^{(1)} - m_b^2 B_1^{(2)} \right) \right],
\end{aligned} \tag{A20}$$

where $\lambda_{ab}^{XY,k} = \lambda_{ai}^{X,k*} \lambda_{bi}^{Y,k}$ with $X, Y = L, R$. The PV-functions are $B_{0,1}^{(l)} = B_{0,1}(p_l^2; m_{n_i}^2, m_{h_k^\pm}^2)$ with $k, l = 1, 2$. In the limit $\theta = 0$, we derived that

$$\begin{aligned}
\text{div}[\bar{a}_l^{nh_1^+ h_1^+}] &= A(m_D m_D^\dagger)_{ba} \times (-t_L), \quad \text{div}[\bar{a}_l^{h_1^+ n n_1}] = 0, \quad \text{div}[\bar{a}_l^{nh_2^+}] = A(m_D m_D^\dagger)_{ba} \times (t_L), \\
\text{div}[\bar{a}_l^{nh_2^+ h_2^+}] &= A(m_D m_D^\dagger)_{ba} \times (-t_W), \quad \text{div}[\bar{a}_l^{h_1^+ n n_1}] = \frac{A(m_D m_D^\dagger)_{ba}}{2s_W c_W}, \quad \text{div}[\bar{a}_l^{nh_2^+}] = A(m_D m_D^\dagger)_{ba} (t_L),
\end{aligned}$$

where $t_L = \frac{s_W^2 - c_W^2}{2s_W c_W}$ satisfy the divergent cancellation for the total amplitudes of LFVZ decays.

-
- [1] T. T. Hong, L. T. T. Phuong, T. P. Nguyen, N. H. T. Nha and L. T. Hue, “ $(g-2)_{e,\mu}$ anomalies and decays $h, Z \rightarrow e_b e_a$ in 3-3-1 models with inverse seesaw neutrinos,” [arXiv:2404.05524 [hep-ph]].
- [2] T. T. Hong, N. H. T. Nha, T. P. Nguyen, L. T. T. Phuong and L. T. Hue, PTEP **2022**, no.9, 093B05 (2022) doi:10.1093/ptep/ptac109 [arXiv:2206.08028 [hep-ph]].

- [3] S. M. Boucenna, J. W. F. Valle and A. Vicente, Phys. Rev. D **92** (2015) no.5, 053001 [arXiv:1502.07546 [hep-ph]].
- [4] A. Abada, J. Kriewald, E. Pinsard, S. Rosauero-Alcaraz and A. M. Teixeira, Eur. Phys. J. C **83** (2023) no.6, 494 [arXiv:2207.10109 [hep-ph]].
- [5] T. T. Hong, Q. D. Tran, T. P. Nguyen, L. T. Hue and N. H. T. Nha, Eur. Phys. J. C **84**, no.3, 338 (2024) [erratum: Eur. Phys. J. C **84**, no.5, 454 (2024)] doi:10.1140/epjc/s10052-024-12692-y [arXiv:2312.11427 [hep-ph]].
- [6] D. Jurčiukonis and L. Lavoura, JHEP **03** (2022), 106 [arXiv:2107.14207 [hep-ph]].
- [7] W. Grimus and L. Lavoura, Phys. Rev. D **66** (2002), 014016 [arXiv:hep-ph/0204070 [hep-ph]].
- [8] P. Abreu *et al.* [DELPHI], Z. Phys. C **73**, 243-251 (1997) doi:10.1007/s002880050313
- [9] R. Akers *et al.* [OPAL], Z. Phys. C **67**, 555-564 (1995)
- [10] G. Aad *et al.* [ATLAS], Phys. Rev. D **90**, no.7, 072010 (2014) [arXiv:1408.5774 [hep-ex]].
- [11] G. Aad *et al.* [ATLAS], Phys. Rev. Lett. **127** (2022), 271801 [arXiv:2105.12491 [hep-ex]].
- [12] G. Aad *et al.* [ATLAS], Phys. Rev. D **108** (2023), 032015 [arXiv:2204.10783 [hep-ex]].
- [13] M. Dam, SciPost Phys. Proc. **1** (2019), 041 [arXiv:1811.09408 [hep-ex]].
- [14] A. Abada *et al.* [FCC], Eur. Phys. J. C **79** (2019) no.6, 474
- [15] T. P. Nguyen, T. T. Le, T. T. Hong and L. T. Hue, Phys. Rev. D **97**, no.7, 073003 (2018) doi:10.1103/PhysRevD.97.073003 [arXiv:1802.00429 [hep-ph]]. [16]
- [16] H. K. Dreiner, H. E. Haber and S. P. Martin, Phys. Rept. **494**, 1-196 (2010) doi:10.1016/j.physrep.2010.05.002 [arXiv:0812.1594 [hep-ph]].
- [17] L. T. Hue, H. T. Hung, N. T. Tham, H. N. Long and T. P. Nguyen, Phys. Rev. D **104**, no.3, 033007 (2021) doi:10.1103/PhysRevD.104.033007 [arXiv:2104.01840 [hep-ph]].
- [18] D. Chang and H. N. Long, Phys. Rev. D **73**, 053006 (2006) doi:10.1103/PhysRevD.73.053006 [arXiv:hep-ph/0603098 [hep-ph]].
- [19] L. Ninh and H. N. Long, Phys. Rev. D **72**, 075004 (2005) doi:10.1103/PhysRevD.72.075004 [arXiv:hep-ph/0507069 [hep-ph]].
- [20] L. T. Hue, H. N. Long, T. T. Thuc and T. Phong Nguyen, Nucl. Phys. B **907**, 37-76 (2016) doi:10.1016/j.nuclphysb.2016.03.034 [arXiv:1512.03266 [hep-ph]].
- [21] V. De Romeri, M. J. Herrero, X. Marcano and F. Scarcella, Phys. Rev. D **95** (2017) no.7, 075028 doi:10.1103/PhysRevD.95.075028 [arXiv:1607.05257 [hep-ph]].
- [22] A. J. Buras, F. De Fazio, J. Girrbach and M. V. Carlucci, JHEP **02**, 023 (2013)

- doi:10.1007/JHEP02(2013)023 [arXiv:1211.1237 [hep-ph]].
- [23] P. A. Zyla *et al.* [Particle Data Group], PTEP **2020**, no.8, 083C01 (2020) doi:10.1093/ptep/ptaa104
- [24] K. Abe *et al.* [T2K], Nature **580**, no.7803, 339-344 (2020) [erratum: Nature **583**, no.7814, E16 (2020)] doi:10.1038/s41586-020-2177-0 [arXiv:1910.03887 [hep-ex]].
- [25] M. Tanabashi *et al.* [Particle Data Group], Phys. Rev. D **98**, no.3, 030001 (2018) doi:10.1103/PhysRevD.98.030001
- [26] R. L. Workman [Particle Data Group], PTEP **2022**, 083C01 (2022)
- [27] B. Aubert *et al.* [BaBar], Phys. Rev. Lett. **104**, 021802 (2010) [arXiv:0908.2381 [hep-ex]].
- [28] A. M. Baldini *et al.* [MEG], Eur. Phys. J. C **76**, no.8, 434 (2016) [arXiv:1605.05081 [hep-ex]].
- [29] A. Abdesselam *et al.* [Belle], JHEP **10**, 19 (2021) doi:10.1007/JHEP10(2021)019 [arXiv:2103.12994 [hep-ex]].
- [30] K. Afanaciev *et al.* [MEG II], Eur. Phys. J. C **84**, no.3, 216 (2024) doi:10.1140/epjc/s10052-024-12416-2 [arXiv:2310.12614 [hep-ex]].
- [31] A. M. Baldini *et al.* [MEG II], Eur. Phys. J. C **78**, no.5, 380 (2018) doi:10.1140/epjc/s10052-018-5845-6 [arXiv:1801.04688 [physics.ins-det]].
- [32] E. Kou *et al.* [Belle-II], PTEP **2019**, no.12, 123C01 (2019) [erratum: PTEP **2020**, no.2, 029201 (2020)] doi:10.1093/ptep/ptz106 [arXiv:1808.10567 [hep-ex]].
- [33] Q. Qin, Q. Li, C. D. Lü, F. S. Yu and S. H. Zhou, Eur. Phys. J. C **78**, no.10, 835 (2018) doi:10.1140/epjc/s10052-018-6298-7 [arXiv:1711.07243 [hep-ph]].
- [34] R. K. Barman, P. S. B. Dev and A. Thapa, Phys. Rev. D **107**, no.7, 075018 (2023) doi:10.1103/PhysRevD.107.075018 [arXiv:2210.16287 [hep-ph]].
- [35] M. Aoki, S. Kanemura, M. Takeuchi and L. Zamakhsyari, Phys. Rev. D **107**, no.5, 055037 (2023) doi:10.1103/PhysRevD.107.055037 [arXiv:2302.08489 [hep-ph]].
- [36] A. M. Sirunyan *et al.* [CMS], Phys. Rev. D **104**, no.3, 032013 (2021) doi:10.1103/PhysRevD.104.032013 [arXiv:2105.03007 [hep-ex]].
- [37] [ATLAS], ATLAS-CONF-2019-037.